Optimal Feedback Switching Control Design for the Turbocharged Diesel Engine with an EGR System

Shashidhar S Gokhale[1*], S. Patil Kulkarni[2], Yathisha L[3*]

[1]Electronics & Communication, Research Scholar, JSSRF, ATME College of Engineering, VTU, Mysuru, India
[2]Electronics & Communication, JSS Science and Technological University, Mysuru, India
[3]Electronics & Communication, ATME College of Engineering, VTU, Mysuru, India

*Corresponding Author: shashisg@gmail.com,   Tel.: +91-9480191567

Abstract— In the present scenario the optimization of engine parameters is very much necessary for the smooth operation of automotive engines. Switching among various strcutures is an essential feature in many engineering applications such as power systems, aircraft systems, etc. This paper presents the intelligent switching technique for the two optimized feedback controllers of the exhaust gas recirculation (EGR) system. The proposed switching control is investigated for the linearized state space model of turbocharged diesel engine with an EGR system. The results are compared with individual feedback structure as well as switching techniques to select the best controller for the future direction.

Keywords— EGR, LQR, Reference input and Optimal Control Theory

I. INTRODUCTION

In internal combustion engines, Exhaust Gas Recirculation (EGR) is a Nitrogen Oxide (NOx) emissions reduction technique used in gasoline/petrol and diesel engines. EGR works by recirculating a portion of an engine's exhaust gas back into the engine cylinders (Engine Manifold) where combustion takes place. This dilutes the Oxygen in the incoming air stream and provides gases inert to combustion to act as absorbent of combustion heat to reduce in cylinder temperature. NOx is produced in a narrow band of high cylinder temperature and pressure.

In a gasoline engine, this inert exhaust displaces the amount of combustible matter in the cylinder. In a diesel engine, the exhaust gas replaces some of the excess oxygen in the pre-combustion mixture. Because NOx forms primarily, when a mixture of nitrogen and oxygen is subjected to high temperature, the lower combustion chamber temperature caused by EGR reduces the amount of NOx the combustion generates with some loss of engine efficiency. Gases reintroduced from EGR systems will also contain near equilibrium concentrations of NOx and CO, the small fraction initially within the combustion chamber inhibits the net production of these and other pollutants when sampled on a time average. Most modern engines now require exhaust gas recirculation to meet emissions standards. Chemical properties of different fuels limit how much EGR may be used. For example methanol is more tolerant to EGR than gasoline.

The EGR control can be divided into open loop and closed loop controls. In open loop control, according to the current conditions and the steady state control MAP (Manifold Absolute Pressure), the EGR valve opening is adjusted by the control system. This control method is simple, but has low precision because the engine operation parameter variation under transient conditions are not considered. In order to improve the control precision, the closed loop EGR control system should be used.

Tianpu Dong , Fujun Zhang , Bolan Liu and Xiaohui An in [1] mentioned that it can be seen from the change trends of the intake oxygen mass fraction and the EGR valve opening that the two algorithms both can achieve accurate tracking of the target value and no overshoot, but the state feedback controller has a shorter adjustment time. The shorter the adjustment time, the quicker will be the change of the NOx emissions and the lower the NOx emissions in the whole control process. Therefore, the control performance of the state feedback controller is better than the PID controller with the step input.

Magdi S. Mahmoud Member, IAENG in [2] has mentioned that Turbocharger increases the power density of the engine by forcing air into the cylinders, which allows injection of additional fuel without reaching the smoke limit. The turbine, which is

driven by the energy in the exhaust gas, has a variable geometry that allows the adaptation of the turbine efficiency based on the engine operating point. The second feedback path from the exhaust to the intake manifold is due to the EGR, which is controlled by the EGR valve. The recirculated exhaust gas replaces oxygen in the inlet charge, thereby reducing the temperature profile of the combustion and hence the emissions of oxides and nitrogen.

Chris Criensy, Frank Willemsy;z, Maarten Steinbuchy y Eindhoven University of Technology, z TNO Automotive, in [3] have mentioned that in order to guarantee robustness properties, apply synthesis framework can be applied to the air path control problem. This model-based approach can deal with the multivariable control problem and can also guarantee optimal performance. Furthermore, it opens the route to a systematic control design procedure, and thus potential for reduced calibration time.

Felipe Castillo Buenaventura, Emmanuel Witrant, Vincent Talon, Luc Dugard in [4] have mentioned that A polytopic LQR controller could be a natural strategy to control system. However, due to the amount of varying parameter as well as the size of the resulting polytope, an LQR gain-scheduled polytopic control or a robust LTI-LQR control give conservative controller gains with poor performance. The implementation can be done by using an Euler method and the calibration of the control can be easily carried out by fixing the ratio between Qu and Ru which is of significant importance for industry-oriented applications.

Jakob Mahler Hansen, Mogens Blanke, Hans Henrik Niemann and Morten Vejlgaard-Laursen in [5] mentioned that the Performance of the EGR control was shown to be satisfactory at low frequencies where current IMO regulations apply, but performance improvement possibilities were shown to be fairly limited if robust sensitivity was a goal under dynamic conditions. The main issues to deal with were shown to be parameter sensitivity of the nonlinear model and the dead time of the primary sensor used for feedback.

The Benjamin Haber, B.S. in [6] mentioned that, Attention must be paid to the robust performance of the controller as computational system identification is inherently inaccurate, due to system nonlinearities, variable transport delay, and other unforeseen dynamics not accounted for in simulation. Intake manifold temperature, pressure, and oxygen mass fraction conditions is highly influential on such low emission combustion modes like low temperature combustion, homogeneous charge compression ignition, and pre-mixed charge compression ignition. These combustion modes have high sensitivity to engine intake conditions and high tendency of knock and misfire, which warrant a comparison of the advanced, multivariable feedback control strategy to conventional feedback control using the complex air-path. Strong benefits to using multivariable control are seen through faster response and settling times along with better disturbance rejection capabilities when maintaining desired intake conditions.

In the following sections, Dynamic Model, State feedback controller design, Switched Linear Control Theory, are described in brief. This is followed by discussion of proposed experiments.

II. DYNAMIC MODEL

The diesel engine system consists of the intake manifold, exhaust manifold, turbocharger, EGR valve, intercooler, EGR cooler and cylinder, as shown in Figure 1.
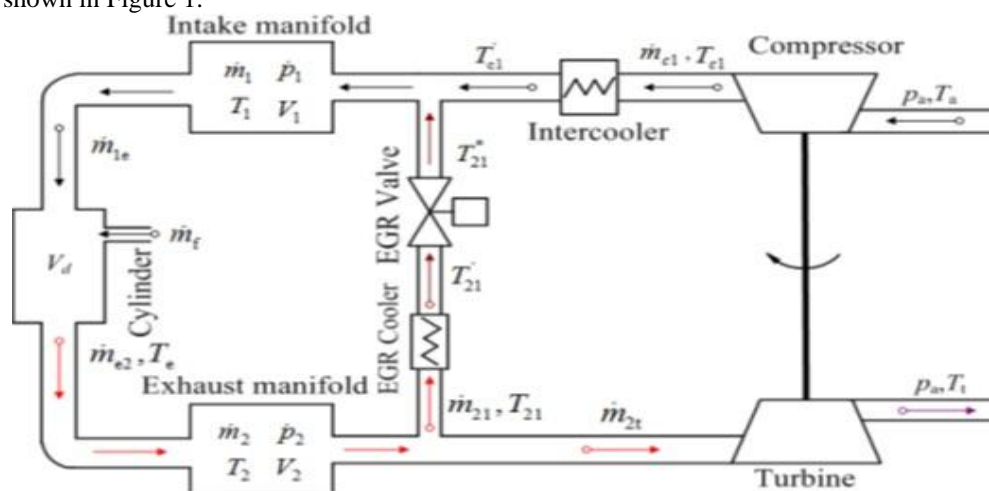

Figure 1: Block diagram of turbocharged diesel engine with HP EGR system.

The analysis of air system can be desribed by seven differential equations

$$\dot{M}_1 = \dot{M}_{c1} + \dot{M}_{21} - \dot{M}_{1e}$$
$$\dot{P}_1 = \frac{\gamma R_g}{V_1}(\dot{M}_{c1}T'_{C1} + \dot{M}_{21}T'_{21} - \dot{M}_{1e}T_1)$$
$$\dot{F}_1 = \frac{\dot{M}_{21}(F_2 - F_1) + \dot{M}_{c1}(1 - F_1)}{M_1}$$
$$\dot{M}_2 = \dot{M}_{e2} - \dot{M}_{21} - \dot{M}_{2t}$$
$$\dot{P}_2 = \frac{\gamma R_g}{V_2}(\dot{M}_{e2}T_e + \dot{M}_{21}T_2 - \dot{M}_{2t}T_2)$$
$$\dot{F}_2 = \frac{\dot{M}_{e2}(F_{e2} - F_2)}{M_2}$$
$$\dot{P}_c = \frac{1}{\tau_{tc}}(n_M P_t - P_c) \tag{1}$$

Tha above model can be simplified by selecting the state variables $x = [P_1, P_2, X_{0,1}, X_{0,2}, P_c]$ and the input variable $u = u_{egr}$, the state space equation of the air system can be derived as:

$$\dot{P}_1 = -K_1 P_1 + K_2 C_d(U_{egr})\Psi_e P_2 + \frac{K_3}{(\pi_c - 1)} P_c \tag{2}$$

$$\dot{P}_2 = K_4 P_1 - [K_5 C_d(U_{egr})\Psi_e + K_6 \Psi_t]P_2 + K_7 \dot{M}_f \tag{3}$$

$$\dot{X}_{0,1} = K_2 C_d(U_{egr})\Psi_e \frac{P_2}{P_1}(X_{0,2} - X_{0,1}) + \frac{K_3}{\pi - 1}\frac{P_c}{P_1}(X_{0,air} - X0,1) \tag{4}$$

$$\dot{X}_{0,2} = K_4 \frac{P_1}{P_2}(X_{0,1} - X_{0,2} - K_7 \dot{M}_f \frac{1}{P_2}(X_{0,2} + l_1) \tag{5}$$

$$\dot{P}_c = K_8 \Psi_t[1 - \pi_t]P_2 - K_9 P_c \tag{6}$$

The intake oxygen mass fraction is chosen as control object that means selecting $X_{0,1}$ as output variable, the output equation is as follows:

$$y = X_{0,1} \tag{7}$$

The state space equations of the air system consists of Equations (2-7) are considered nonliner. By applying Taylor approximation linearization method, the non linear model can be linearized as follows:

$$\Delta \dot{x} = A\Delta x + B\Delta u \tag{8}$$
$$\Delta y = C\Delta x + D\Delta u \tag{9}$$

where, $\Delta x = x - x_0$, $\Delta u = u - u_0$, and $\Delta y = y - y_0$; A, B, C, D are the coefficient matrices of the state space model, which can be derived as follows:

$$A = \left(\frac{\partial f}{\partial x^T}\right)_{x_0, u_0} = \begin{bmatrix} \frac{\partial f_1}{\partial P_1} & \frac{\partial f_1}{\partial P_2} & 0 & 0 & \frac{\partial f_1}{\partial P_c} \\ \frac{\partial f_2}{\partial P_1} & \frac{\partial f_2}{\partial P_2} & 0 & 0 & 0 \\ \frac{\partial f_3}{\partial P_1} & \frac{\partial f_3}{\partial P_2} & \frac{\partial f_3}{\partial X_{0,1}} & \frac{\partial f_3}{\partial X_{0,2}} & \frac{\partial f_3}{\partial P_c} \\ \frac{\partial f_4}{\partial P_1} & \frac{\partial f_4}{\partial P_2} & \frac{\partial f_4}{\partial X_{0,1}} & \frac{\partial f_4}{\partial X_{0,2}} & 0 \\ 0 & \frac{\partial f_5}{\partial P_2} & 0 & 0 & \frac{\partial f_5}{\partial P_c} \end{bmatrix}_{x_0, u_0}$$

$$B = (\frac{\partial f}{\partial u})_{x_0,u_0} = \begin{bmatrix} \dfrac{\partial f_1}{\partial u_{egr}} \\ \dfrac{\partial f_2}{\partial u_{egr}} \\ \dfrac{\partial f_3}{\partial u_{egr}} \\ 0 \\ 0 \end{bmatrix}_{x_0,u_0}$$

III.STATE FEEDBACK CONTROLLER DESIGN

The state feedback controllers for this paper are designed using the optimal control theory of linear quadratic regulator algorithm (LQR) [7]. A special case of optimal control problem which is of particular importance arises when the objective function is a quadratic function of x and u, and the dynamic equations are linear. The resulting feedback law in this case is known as the linear quadratic regulator (LQR). The LQR controller generates the parameters of the gain by minimizing the error criteria in Eqn.(10). Consider a linear system characterized by Eq's (8,9) where (A, B) is stabilizable. Then the cost index that determines the matrix K of the LQR vector is

$$J = \tfrac{1}{2}\int_0^\infty (x^T Q x + u^T R u)dt \tag{10}$$

Where Q and R are the positive-definite Hermitian or real symmetric matrices. From the above equations,

$$K = -R^{-1}B^T P \tag{11}$$

and hence the control law is,

$$u(t) = -Kx(t) = -R^{-1}B^T Px(t) \tag{12}$$

In which P must satisfy the reduced Riccati equation:

$$PA + A^T P - PBR^{-1} + B^T P + Q = 0 \tag{13}$$

The LQR function allows you to choose two parameters, R and Q, which will balance the relative importance of the input and state in the cost function that you are trying to optimize. Essentially, the LQR method allows for the control of all outputs.

The feedback gain matrix K with the different weighted coefficients Q and R around the operating point can be analyzed with the following results:

1. $Q = I$, $R = 3$

$$K_1' = \begin{bmatrix} 4.82 * 1.0e - 07 \\ 1.07 * 1.0e - 06 \\ -0.41 \\ -5.5 * 1.0e - 03 \\ -7.70 * 1.0e - 05 \end{bmatrix}$$

2. $Q = I$, $R = 20$

$$K_2' = \begin{bmatrix} 1.13 * 1.0e - 07 \\ 2.44 * 1.0e - 07 \\ -0.1 \\ -1.8 * 1.0e - 03 \\ -3.46 * 1.0e - 03 \end{bmatrix}$$

3. $Q = I$, $R = 30$

$$K_3' = \begin{bmatrix} 7.75 * 1.0e - 08 \\ 1.69 * 1.0e - 07 \\ -0.07 \\ -1.3 * 1.0e - 03 \\ -2.67 * 1.0e - 05 \end{bmatrix}$$

The three optimized state feedback controllers K_1, K_2 & K_3 are subjected to optimal switching strategies in the combination of switch K_1/K_2, K_2/K_3 & K_3/K_1 combinations and the results are also compared for without switching (individual feedback structures).

IV. SWITCHED LINEAR CONTROL THEORY

A switched system is a dynamical system that consists of a finite number of subsystems and a logical rule that orchestrates switching between these subsystems. Hybrid or switching systems, commonly found in control theory which are characterised by a combination of both continous & discrete systems. The performance of these systems can be realised by switching between relatively two simple linear time invariant (LTI) systems with different control techniques [8-11].

The advantage of switching between different feedback structures is to combine the useful properties of each structure and to introduce new properties that are not present in any of the structures used.

Zhi Hong Huang & Cheng Xiang in [12] derived a necessary and sufficient condition for stability of arbitrarily switched second order LTI systems with marginally stable subsystems. It turns out that the condition for the marginally stable case is similar with the one for asymptotically stable except boundary conditions are included. The performance based switching algorithm for LTI systems based on Lyapunov stability criteria was developed by [13]. Hussain N & Al-Duwaish in [14] have proposed an adaptive neural network based Sliding Mode Control (SMC) for a power system stsbilizer (PSS) of a single machine power system. The SMC is essentially a switching feedback control. Simulation results indicate that the controller performance is greatly improved by the use of adaptive SMC.

The LTI switched systems have found many applications in the areas such as aircraft, robotics, power system, etc. In the context of automotive electronics, Switched system has very broad applications. Rapid development of parameters in the engine modeling resluts in decrease of system performance. In order to overcome this drawback, switching between two feedback structure is very much needful to fulfill the todays requirement to automatically select the best feedback structure for the system depending upon the operating conditions, evironmental constraints etc.

A switched-linear system model for the current research is as follows (refer Figure 2):

$$\dot{x} = A_\sigma x(t) \tag{14}$$

The switching signal $\sigma(t)$ indicates

$$\dot{x}(t) = A_\alpha x(t) = if, \quad \sigma = \alpha \tag{15}$$
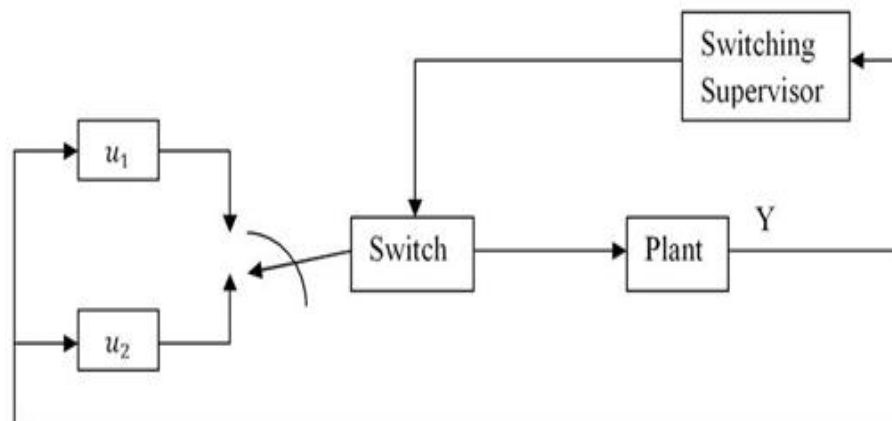$$= A_\beta x(t) = if, \quad \sigma = \beta$$

Figure 2: General switched linear system

4.1 Switching Control Algorithm

A switching control algorithm that minimizes output energy and also shown to be stabilizing is presented in [15] & [16]. Design of this performance based switching control law is equivalent to finding a switching matrix S that depends on state of the system. The Algorithm is as follows:

1. Initialize the two closed loop systems A_α & A_β.

2. Determine T_0 by solving the algebraic Lyapunov Equation:

$$A_\alpha^T T_0 + T_0 A_\alpha = -C^T C$$

3. Using, A_2 define the switching matrix:

$$S = -(A_\beta^T T_0 + T_0 A_\beta + C^T C)$$

4. Now, the switching rule is,

$$\sigma = \beta \, if \, \ll x, Sx \gg > 0$$
$$= \alpha \, otherwise$$

4.2 Optimization of Performance Indices Via Switching Control

The optimization of performance index J is measured by the following equation:

$$J_{Switch} \leq min(J_1, J_2) \tag{16}$$

Where, J_1 & J_2 are the performance index of two subsystems A_α & A_β, where switching takes place between these two subsystems.

4.3 Switching control strategies

The switching control strategies are developed for the following three cases and the numerical calculated switching matrices values are as follows:

4.3.1 Case I

Switch K_1/K_2: In this case A_α & A_β are defined as follows:
$$A\alpha = A - BK_1$$
$$A\beta = A - BK_2$$

4.3.2 Case II

Switch K_2/K_3: In this case A_α & A_β are defined as follows:
$$A\alpha = A - BK_2$$
$$A\beta = A - BK_3$$

4.3.3 Case III

Switch K_3/K_1: In this case A_α & A_β are defined as follows:
$$A\alpha = A - BK_3$$
$$A\beta = A - BK_1$$

4.4 Reference Input Design With Full State Feedback

The need for the design of reference input and to introduce into the engine modeling system is to get the knowledge about the transient response of the pole placement designs.
The control law is given by,

$$u = -Kx + r \tag{17}$$

Where, r is the reference input to the system.

From, Eq. 13, it is almost clear that the system will have nonzero steady state error for the step input. In order to overcome this, let us define the control input as

$$u = u_{SS} - K(x - x_{SS}) \tag{18}$$

Where, u_{SS} & x_{SS} are the desired final values of the state and the control input. When, $x = x_{SS}$ (no error), $u = u_{SS}$. The system differential equations are given by,

$$\dot{x} = Ax + Bu \tag{19}$$

$$y = Cx + Du \tag{20}$$

In the constant steady state, Eq's (15) & (16) reduce to the pair

$$0 = Ax_{SS} + Bu_{SS} \tag{21}$$

$$y = Cx_{SS} + Du_{SS} \tag{22}$$

The gain calculation for the reference input is given by,

$$\begin{bmatrix} A & B \\ C & D \end{bmatrix} \begin{bmatrix} N_x \\ N_u \end{bmatrix} = \begin{bmatrix} 0 \\ 1 \end{bmatrix}$$

$$\begin{bmatrix} N_x \\ N_u \end{bmatrix} = \begin{bmatrix} A & B \\ C & D \end{bmatrix}^{-1} \begin{bmatrix} 0 \\ 1 \end{bmatrix}$$

The reference input gain N' is given by,

$$\bar{N} = N_u + KN_x \tag{23}$$

The numerical values of $\bar{N}$ for the individual controllers (K_1, K_2,&K_3) are shown in Table I.

Table 1: Reference Input Gain $\bar{N}$ values for proposed optimal controllers

Feedback Controller	ΔP_1	ΔP_2
K_1	-0.00012179	-0.00012179
K_2	-5.6226*1.0e-05	-5.6226*1.0e-05
K_3	-4.95759*1.0e-05	-4.95759*1.0e-05

The numerical values of $\bar{N}$ for the switching between feedback controllers in different cases are taken as average between two relevant feedback controllers and are shown in Table 2:

$$\bar{N}(S12) = \frac{\bar{N}(K_1) + \bar{N}(K_2)}{2} \tag{24}$$

$$\bar{N}(S23) = \frac{\bar{N}(K_2) + \bar{N}(K_3)}{2} \tag{25}$$

$$\bar{N}(S31) = \frac{\bar{N}(K_1) + \bar{N}(K_3)}{2} \tag{26}$$

Table 2: Reference Input Gain $\bar{N}$ values for proposed switching techniques

Feedback Controller	ΔP_1	ΔP_2
$S12$	-8.90089*1.0e-05	-8.90089*1.0e-05
$S23$	-5.29012*1.0e-05	-5.29012*1.0e-05
$S31$	-8.56836*1.0e-05	-8.56836*1.0e-05

V. SIMULATION RESULTS

The experimental set-up to test the proposed control techniques consists of dynamic state space model described by A and B matrices below:

$$A = \begin{bmatrix} -130.64 & 8.91 & 0 & 0 & 1538.1 \\ 92.05 & -212.84 & 0 & 0 & 0 \\ -3.99*10^{-5} & -8.25*10^{-4} & -17.72 & 1.41 & 0.013 \\ 0.0047 & 1.80*10^{-4} & 50.84 & -52.50 & 0 \\ 0 & 2.32 & 0 & 0 & -33.33 \end{bmatrix}$$

$$B = \begin{bmatrix} 1.02*10^6 \\ -4.64*^6 \\ -94.81 \\ 0 \\ 0 \end{bmatrix}$$

The numerical values of the proposed switching matrices for the state variables $\dot{P}_1\&\dot{P}_2$ are also shown for the three cases:

5.1 Case I
Switch K_1/K_2: The switching matrix defined for this case as S_{12} :

$$S_{12}(\dot{P}_1) = \begin{bmatrix} -0.001 & -0.001 & 461.06 & 5.49 & 0.0811 \\ -0.001 & 0.0010 & -201.772 & -2.418 & 0.0129 \\ 461.06 & -201.77 & 4307793.4 & 55307.94 & -14612.3 \\ 5.49 & -2.418 & 55307.94 & 706.58 & -173.87 \\ 0.08 & 0.0129 & -14612.34 & -173.87 & -4.077 \end{bmatrix}$$

$$S_{12}(\dot{P}_2) = \begin{bmatrix} 0.0010 & 0.004512 & -458.002 & 5.412 & -0.065 \\ 0.00451 & 0.0148 & -2805.64 & -33.36 & -0.3908 \\ -458.02 & -2805.64 & 1507244 & 134921.7 & 4735.89 \\ -5.412 & -33.3668 & 134921.7 & 1073.55 & 50.373 \\ -0.065 & -0.39086 & 4735.89 & 50.3737 & 1.0135 \end{bmatrix}$$

5.2 Case II
Switch K_2/K_3: The switching matrix defined for this case as S_{23} :

$$S_{23}(\dot{P}_1) = \begin{bmatrix} -0.0011 & -0.001 & 461.06 & 5.49 & 0.0811 \\ -0.0010 & 0.0010 & -201.772 & -2.418 & 0.0129 \\ 461.06 & -201.77 & 4307793.4 & 55307.94 & -14612.34 \\ 5.49 & -2.418 & 55307.94 & 706.58 & -173.87 \\ 0.08 & 0.0129 & -14612.34 & -173.87 & -4.077 \end{bmatrix}$$

$$S_{23}(\dot{P}_2) = \begin{bmatrix} 0.00106 & 0.004512 & -458.002 & 5.412 & -0.065 \\ 0.004512 & 0.0148 & -2805.64 & -33.3668 & -0.39086 \\ -458.02 & -2805.64 & 1507244 & 134921.7 & 4735.89 \\ -5.412 & -33.3668 & 134921.7 & 1073.55 & 50.373 \\ -0.065 & -0.39086 & 4735.89 & 50.3737 & 1.0135 \end{bmatrix}$$

5.3 Case III

Switch K_3/K_1: The switching matrix defined for this case as S_{31} :

$$S_{31}(\dot{P}_1) = \begin{bmatrix} -0.0011 & -0.001 & 461.06 & 5.49 & 0.0811 \\ -0.0010 & 0.0010 & -201.772 & -2.418 & 0.0129 \\ 461.06 & -201.77 & 4307793.4 & 55307.94 & -14612.34 \\ 5.49 & -2.418 & 55307.94 & 706.58 & -173.87 \\ 0.08 & 0.0129 & -14612.34 & -173.87 & -4.077 \end{bmatrix}$$

$$S_{31}(\dot{P}_2) = \begin{bmatrix} 0.00106 & 0.004512 & -458.002 & 5.412 & -0.065 \\ 0.004512 & 0.0148 & -2805.64 & -33.3668 & -0.39086 \\ -458.02 & -2805.64 & 1507244 & 134921.7 & 4735.89 \\ -5.412 & -33.3668 & 134921.7 & 1073.55 & 50.373 \\ -0.065 & -0.39086 & 4735.89 & 50.3737 & 1.0135 \end{bmatrix}$$

To validate the comparison and effectiveness of proposed switching controllers the simulations are carried for the state variables Intake manifold pressure deviation ($\Delta\dot{P}_1$) and Exhaust manifold pressure deviation ($\Delta\dot{P}_2$). Figures 3-4, show the case I (Switch K_1/K_2) responses, Figures 5-6, reveal the case II (Switch K_2/K_3) responses and Figures 7-8, indicate the case III (Switch K_3/K_1) responses of the state variables ($\Delta\dot{P}_1$ and $\Delta\dot{P}_2$. Figures 9-14, shows the switching signal responses of three cases.
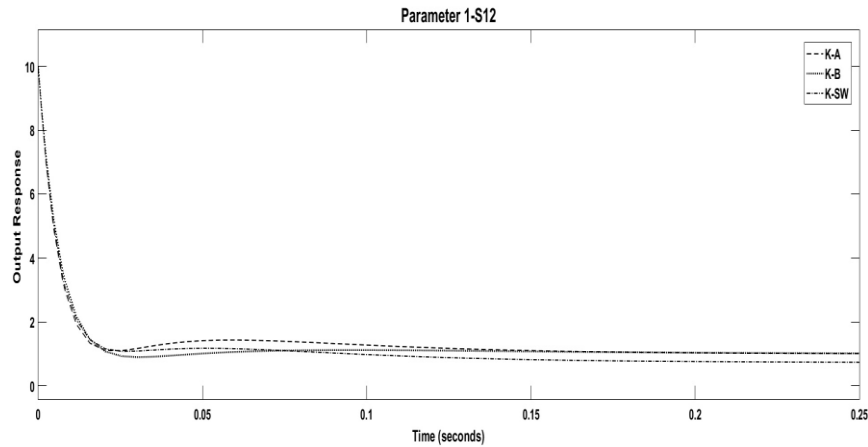

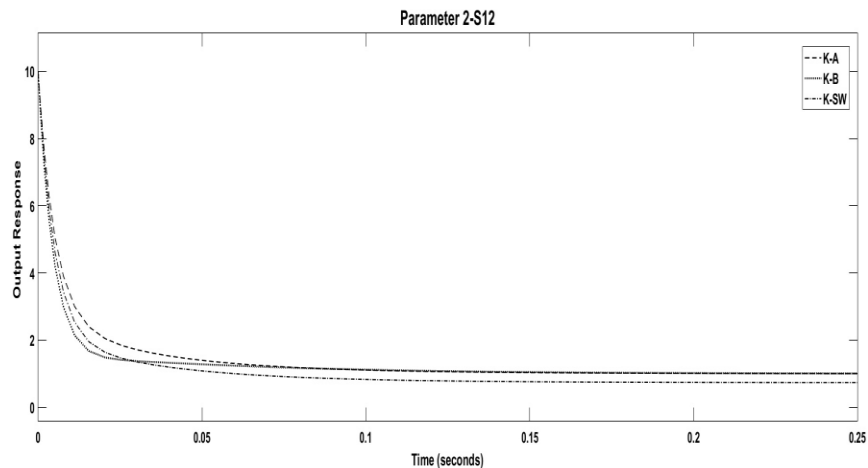Figure 3: Case I Response of $\Delta\dot{P}_1$

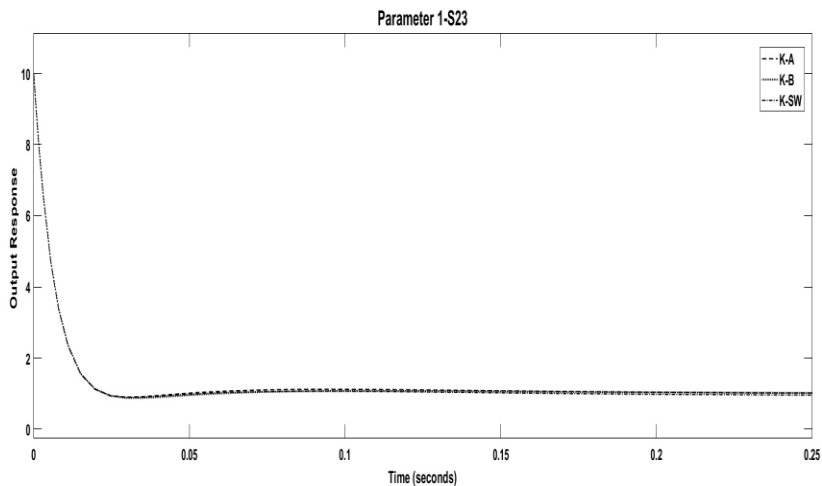Figure 4: Case I Response of $\Delta\dot{P}_2$

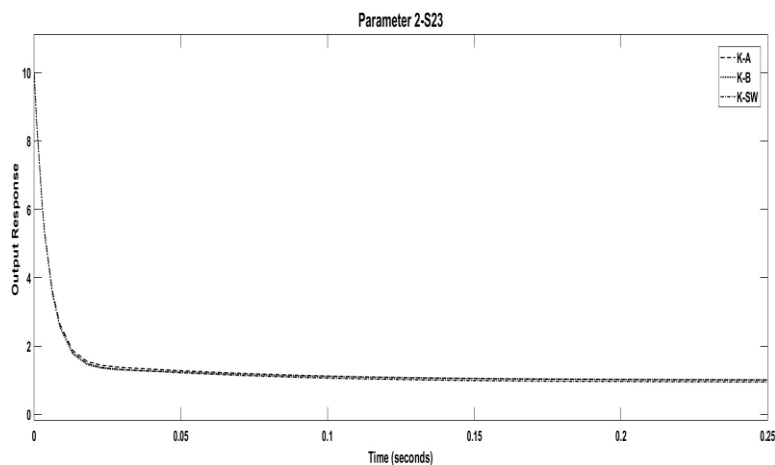Figure 5: Case II Response of $\Delta \dot{P}_1$

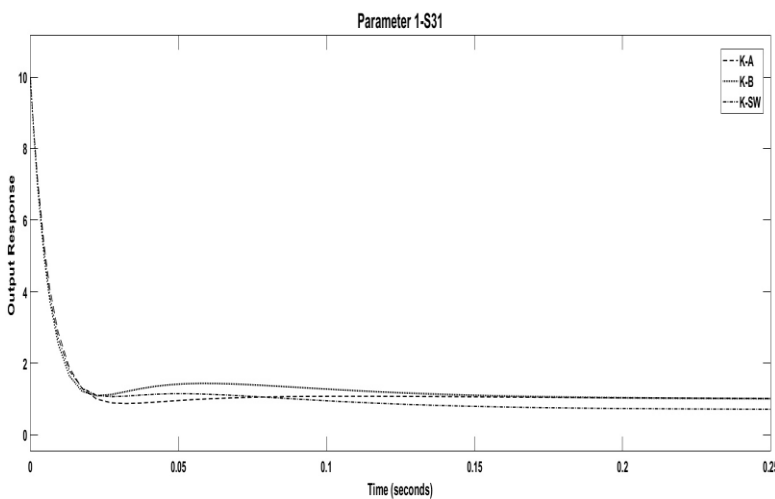Figure 6: Case II Response of $\Delta \dot{P}_2$

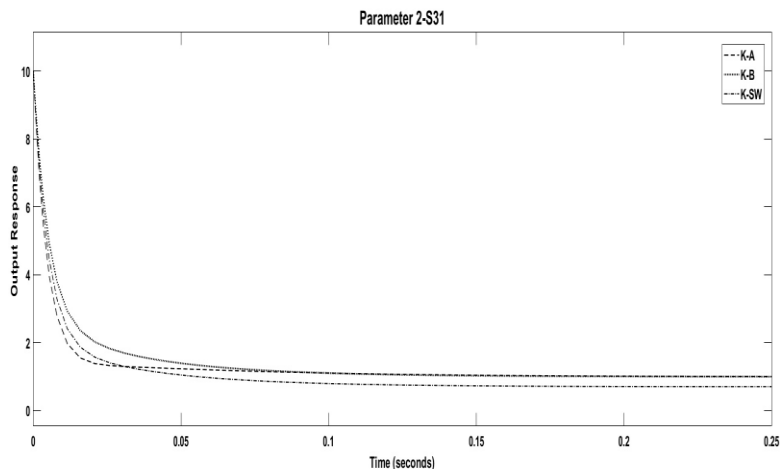Figure 7: Case III Response of $\Delta \dot{P}_1$

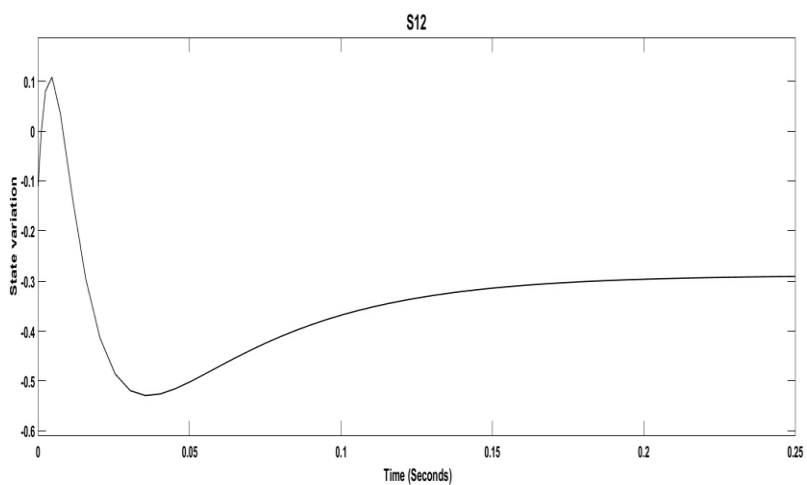Figure 8: Case III Response of $\Delta \dot{P}_2$

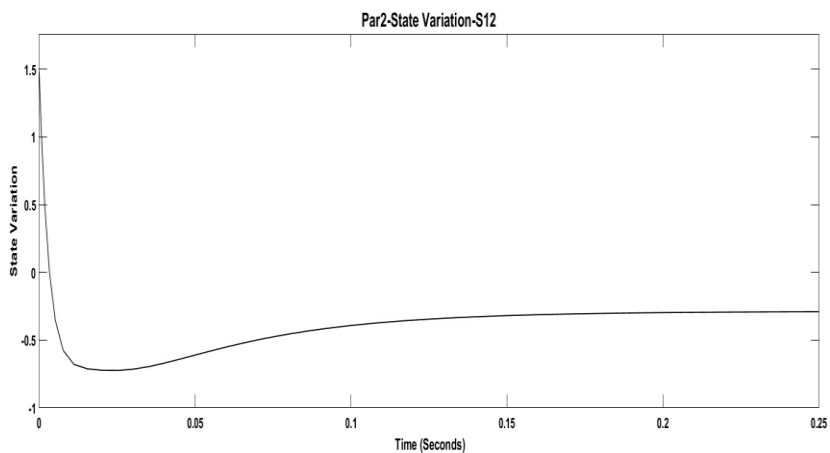Figure 9: Case I Switching Signal Response of $\Delta \dot{P}_1$

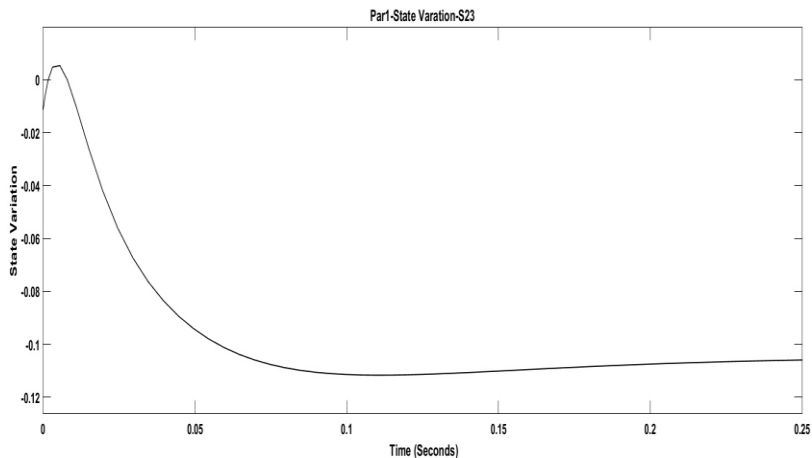Figure 10: Case I Switching Signal Response of $\Delta \dot{P}_2$
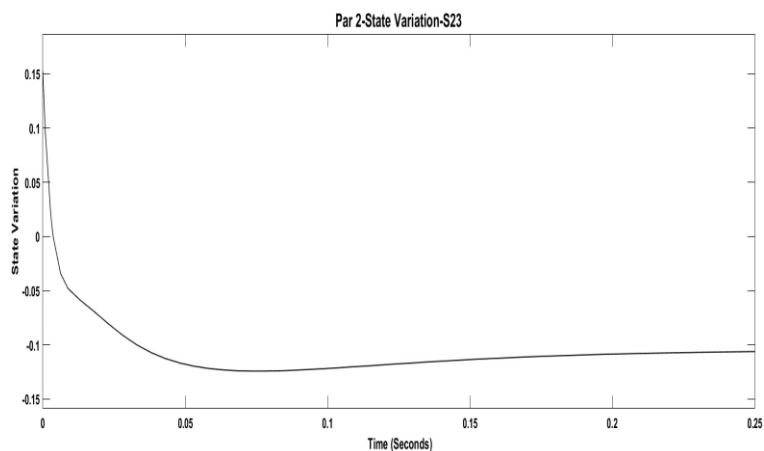
Figure 11: Case II Switching Signal Response of $\Delta\dot{P}_1$

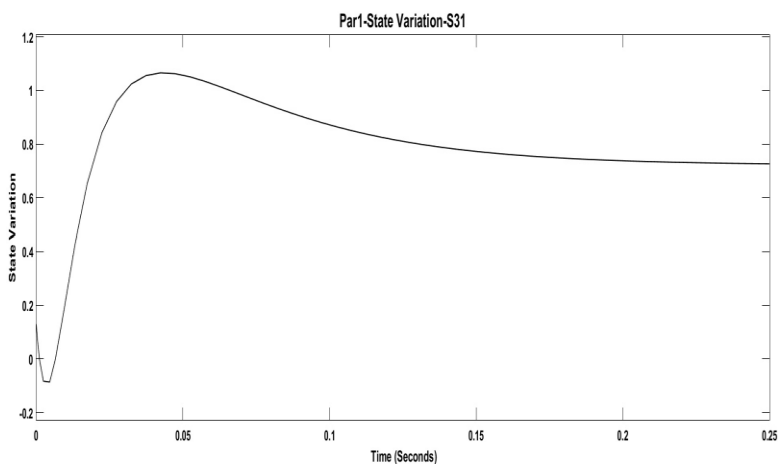Figure 12: Case II Switching Signal Response of $\Delta\dot{P}_2$

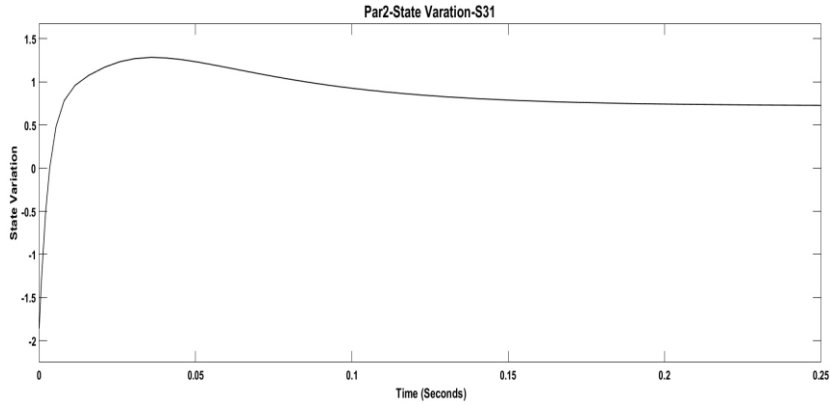Figure 13: Case III Switching Signal Response of $\Delta\dot{P}_1$

Figure 14: Case III Switching Signal Response of $\Delta \dot{P}_2$

VI. DISCUSSION

The simulation results of all the cases for two state variables indicates the switching taking palce between K_1/K_2 (Case I), K_2/K_3 (Case II), K_3/K_1 (Case III). The results reveal that the switching between two optimal feedback controllers has better improved performance in all the three cases compared to the individual optimal feedback controllers (without switching) with respect to settling time and eventhough switching peak overshoots are not too high. Table III, shows the comparison results of settling time for with and without switching control techniques. Table IV, shows the peak overshoots value for the three cases of switching. Table V, shows the comparison of performance index J for with and without optimal switching techniques and it reveals that the switching between two individual optimal feedback control techniques as better optimization compared to without switching.

Table 3: Comparison of settling time (T_S) (in seconds) for State Variables

State Variable	$K1$	$K2$	$SwitchK1/K2(S12)$
ΔP_1	0.08	0.075	0.025
ΔP_2	0.03	0.07	0.025

State Variable	$K2$	$K3$	$SwitchK2/K3(S23)$
ΔP_1	0.13	0.13	0.12
ΔP_2	0.13	0.13	0.12

State Variable	$K3$	$K1$	$SwitchK3/K1(S31)$
ΔP_1	0.075	0.1	0.02
ΔP_2	0.03	0.1	0.025

Table 4: Comparison of Peak Overshoot (M_P) of Switching matrices for State Variables

State Variable	$S12$	$S23$	$S31$
ΔP_1	0.45	0.103	-0.9
ΔP_2	1.75	0.25	0.5

Table 5: Comparison of Performance Index (J) for State Variables

State Variable	$K1$	$K2$	$SwitchK1/K2(S12)$
ΔP_1	0.662	0.625	0.5514
ΔP_2	0.7313	0.6059	0.5396

State Variable	$K2$	$K3$	$SwitchK2/K3(S23)$
ΔP_1	0.625	0.6158	0.6027
ΔP_2	0.6058	0.5871	0.5703

State Variable	$K3$	$K1$	$SwitchK3/K1(S31)$
ΔP_1	0.6158	0.662	0.542
ΔP_2	0.5872	0.7313	0.5226

VII. CONCLUSION

Switching strategies have been an effective control tool used in such popular methods as optimal control. In this paper, it is shown that the optimal switching feedback control technique for turbo charged diesel engine has less optimization compared to the coventional control techniques (without switching). The optimal switching idea has been proposed in this paper for three different cases and the MATLAB simulation results are compared. The results conclude that the case III, techniques provides lesser optimization compared to other two cases (caseI & case II).

ACKNOWLEDGMENT

REFERENCES

[1]   Tianpu Dong, Fujun Zhang, Bolan Liu and Xiaohui "An Model-Based State Feedback Controller Design for a Turbocharged Diesel Engine with an EGR System*"*, energies, ISSN 1996-1073, www.mdpi.com/journal/energies.
[2]   Magdi S. Mahmoud Member, IAENG "Improved Controller Design for Turbocharged Diesel Engine", Proceedings of the World Congress on Engineering 2012 Vol III, WCE 2012, July 4 - 6, 2012, London, U.K.
[3]   Chris Criensy, Frank Willemsyz, Maarten Steinbuchy, Eindhoven University of Technology, TNO Automotive "A Systematic Approach Towards Automated Control Design for Heavy-Duty EGR Diesel Engines" .
[4]   Felipe Castillo Buenaventura, Emmanuel Witrant, Vincent Talon, Luc Dugard "Air Fraction and EGR Proportion Control for Dual Loop EGR Diesel Engines*"*, Ingenieria y Universidad, Pontifica Universidad Javeriana, Faculty of Science, 2015, 19 (1), pp.115 - 133. <10.11144/Javeriana.iyu19-1.aegr>. <hal-01222866>.
[5]   Jakob Mahler Hansen, Mogens Blanke, Hans Henrik Niemann, Morten Vejlgaard, Laursen "Exhaust Gas Recirculation Control for Large Diesel Engines, Achievable Performance with SISO Design".
[6]   Benjamin Haber, B.S.*A* "Robust Control Approach on Diesel Engines with Dual-Loop Exhaust Gas Recirculation Systems*"*, Thesis, The Ohio State University, 2010. <hal-01222866>.
[7]   Yathisha L and S Patil Kulkarni. "Optimum LQR Switching Approach for the Improvement of STATCOM Performance", *Springer LNEE*, Vol 150, E-ISSN: 1876-1100, 2013, pp. 259-266, DOI: 10.1007/978-1-4614-3363-7_28.
[8]   Hamid Niyazi and Fakhralsadat Rastegari, "Design of A Novel Resistive Capacitive Feedback Trans-impedance Amplifier", International Journal of Computer Sciences and Engineering, Vol.-4(6), PP(01-07) Jun 2016, E-ISSN: 2347-2693.
[9]   Keith R. Santarelli and Munther A. Dahleh. "Comparison between a switching controller and two LTI controllers for a class of LTI plants", *International Journal on Robust Nonlinear Control*, 2008, pp. 1-33, DOI: 10.1002/rnc.1308.
[10]   Keith R. Santarelli and Munther A. Dahleh. "L2 Gain Stability of Switched Output Feedback Controllers for a Class of LTI Systems", *IEEE Transactions on Automatic Control*, VOL. 54, NO. 7, July 2009, pp. 1504-1514.
[11]   Keith R. Santarelli and Munther A. Dahleh. "Optimal controller synthesis for a class of LTI systems via switched feedback", *Systems & Control*

Letters, Elsevier Journal, VOL. 59, Issue No. 3, March 2010, pp. 258-264.

[12] Zhi Hong Huang, Cheng Xiang, Hai Lin and Tong Heng Lee. "A Necessary and Sufficient Condition for Stability of Arbitrarily Switched Second-Order LTI System: Marginally Stable Case", *22nd IEEE International Symposium on Intelligent Control Part of IEEE Multi-conference on Systems and Control*, Singapore, 1-3 October 2007, pp. 83-88.

[13] Jorge L. Aravena and Lalitha Devarakonda. "Performance Driven Switching Control", *IEEE Transactions on Industrial Electronics*, 2006, July 9-12, 2006, pp. 31-36.

[14] Hussain N. Al-Duwaisha and Zakariya M. Al-Hamouz. "A Neural Network Based Adaptive Sliding Mode Controller: Application to a Power System Stabilizer", *Elsevier Proceedings, Energy Conversion and Management*, Volume 52, Issue 2, February 2011, Pp. 1533-1538.

[15] Yathisha L, Kourosh Davoodi and S Patil Kulkarni. "Optimal switching control strategy for UPFC for wide range of operating conditions in power system", *3rd Indian Control Conference*, IEEE Xplore, Jan 2017, Indian Institute of Technology (IIT), Guwhati, pp 225-232. DOI:10.1109/INDIANCC.2017.7846479.

[16] Yathisha L and S Patil Kulkarni. "Application and comparison of switching control algorithms for power system stabilizer", *IEEE International Conference on Industrial Instrumentation and Control (ICIC)*, IEEE Xplore, May 2015, Pune, pp 1300-1305. DOI:10.1109/IIC.2015.7150949.

Authors' Profile

Mr. Shashidhar S Gokhale obtained Masters Degree in Industrial Electronics from NITK, Surathkal, Mysore University in the year 1983. Presently he is working towards Doctoral Degree in Electronics, in the field of control systems in the prestigious Mysore University, India. He has been working as an Associate Professor in the department of Electronics and Communication Engineering, ATME, Mysore, since 2012. He has 25 years of industrial experience and 8 years of teaching experience in various industries and colleges in India as well as Singapore. Email: shashisg@gmail.com

Dr. Sudarshan S Patil Kulkarni received his Ph.D. degree from Old Dominion university, Norfolk, Virginia, USA in 2004. He is currently working as Professor in the Department of Electronics & Communication at Sri Jayachamarajendra College of Engineering (SJCE), JSS Science & Technology University, Mysore, INDIA. His research interests include control systems, hybrid & stochastic systems, VLSI, signal & image processing. E-mail: pk.sudarshan@gmail.com.

Dr. Yathisha L. received his Doctoral Degee in Control Systems & Masters Degree in Industrial Electronics from SJCE, Visvesvaraya Technological University(VTU) in the year 2017 & 2010 respectively. Since 2012 He has been working as Associate Professor in the Department of Electronics & Communication Engineering, ATME College of Engineering (affiliated to VTU), Mysore, INDIA. His areas of interests are Power Systems, Control Systems and Hybrid Control Systems. E-mail: yathisha.171@gmail.com.